Antitumor Effects and Blood Flow Dynamics After Photodynamic Therapy using Benzoporphyrin Derivative Monoacid Ring A in KLN205 and LM8 Mouse Tumor Models

Tomohiro Osaki, Satoshi Takagi, Yuki Hoshino, Masahiro Okumura, Toru Fujinaga

Laboratory of Veterinary Surgery, Department of Veterinary Clinical Sciences,
Graduate School of Veterinary Medicine, Hokkaido University, Sapporo, Hokkaido
Kita 18, Nishi 9, Kita-ku, Sapporo, 060-0818, Japan

CORRESPONDENCE TO:

Tomohiro Osaki, DVM
Laboratory of Veterinary Surgery,
Department of Veterinary Clinical Sciences,
Graduate School of Veterinary Medicine, Hokkaido University
Kita 18, Nishi 9, Kita-ku, Sapporo, 060-0818, Japan

E-mail: ohchan@vetmed.hokudai.ac.jp
TEL +81-11-706-5230
FAX +81-11-706-5229

Summary

Photodynamic therapy (PDT) using benzoporphyrin derivative monoacid ring A (BPD-MA) induces direct tumor cell damage and microvascular injury. We administered BPD-MA at 3 h or 15 min before laser irradiation to KLN205 and LM8 tumors in murine models. Tumor growth delay was induced more effectively by 15-min-interval PDT than by 3-h-interval PDT. Vascularity and blood perfusion was significantly decreased by 15-min-interval PDT. We observed death of all tumor cells, except peripheral cells, in the 3-h-interval PDT group, and death of cells around the damaged tumor vasculature in the 15-min-interval PDT group. Thus, 15-min-interval-PDT enhanced the antitumor effect by damaging tumor vasculature.

1. Introduction

Photodynamic therapy (PDT) is a more selective method for cancer treatment than either chemotherapy or radiation therapy, because tumor tissue damage occurs only when a photosensitizer, molecular oxygen, and light of an appropriate wavelength are simultaneously presented to the tumor area. Upon photoactivation, reactive oxygen species are generated; these have a short lifetime (<0.04 s) and a short radius of action (<0.02 μm), and induce irreversible damage to the cells in the microenvironment [1,2]. PDT targets the tumor cells, the tumor bed microvasculature as well as normal microvasculature, and the inflammatory and immune host system. It was considered that targeting a combination of all these components is required for long-term tumor control [3].

Benzoporphyrin derivative monoacid ring A (BPD-MA) is a second generation photosensitizer with rapid body clearance and strong light absorption at a wavelength of approximately 690 nm; this wavelength enables considerably high light penetration into the tissue [4]. This photosensitizer has been approved for the treatment of age-related macular degeneration and is under investigation for the treatment of tumors. In cases of high accumulation of the photosensitizer in tumor cells, cellular-targeting PDT (3-h-interval PDT) was generally performed at 3 h after BPD-MA administration. Therefore, slight hemostasis was observed in the 3-h-interval PDT group [5]. On the other hand, in cases of high accumulation of photosensitizer in tumor vasculature, vasculature-targeting PDT (15-min-interval PDT) was performed at 15 min after BPD-MA administration. Therefore, vascular damage and hemostasis was observed in the 15-min-interval PDT group [5].

Photoactivation of BPD-MA when it is largely localized within the blood vessels damages the microvasculature endothelium [6,7]. In tumor tissue, microvasculature

damage is readily observed histologically following PDT; this damage leads to a significant decrease in blood flow as well as severe and persistent hypoxia [8-11]. The treatment-induced reaction of the tumor vasculature can determine the prognosis, and it can be assessed by the histological examination of the tumor. Since, this method requires obtaining tissue samples repeatedly by invasive biopsy, it is impractical. A number of techniques have been reported for imaging the blood vessels in solid tumors invasively and repeatedly [12,13]. Among these, power Doppler ultrasound (US) could noninvasively monitor the tumor blood flow [12]. Therefore, this method could enable the assessment of the vascularity and blood perfusion within the tumor tissue after PDT.

In addition, it was reported that PDT produced microvascular damage within the treated tumors, and the resulting tumor hypoxia induced a number of molecular and physiological responses, including an adaptive response associated with gene activation [14,15]. A primary step in hypoxia-mediated gene activation is the formation of the hypoxia-inducible factor-1 (HIF-1) transcription factor complex [14,16], which is a heterodimeric complex of two helix-loop-helix proteins, HIF-1α and HIF-1β [17]. However, in PDT using BPD-MA, little is known about the correlation between PDT-induced antivascular effects and tumor cell reactions to the resulting hypoxia within the tumor tissue.

In this study, we investigated the antitumor effect, tumor blood flow dynamics, and hypoxia after the 3-h-interval PDT and the 15-min-interval PDT using BPD-MA in KLN205 and LM8 mouse tumor models. The effects of PDT on local tumor control were evaluated by a histological study and a tumor regrowth assay. The time course of changes in the blood flow after PDT was monitored by a power Doppler US. Furthermore, western blot analysis was performed to assess whether PDT-induced hypoxia could lead to an increase in hypoxia-inducible factor-1α (HIF-1α) expression

within the treated tumor tissue.

2. Materials and Methods

2.1. Tumor cell lines and cell culture *in vitro*

KLN205 cells were obtained from the Institute of Development, Aging and Cancer, Tohoku University (Miyagi, Japan). KLN205 tumor cells were established from the Nettesheim lung carcinoma in mice (transplantable to DBA/2 mouse) [18]. LM8 cells were obtained from RIKEN BioResource Center (Ibaraki, Japan). LM8 tumor cell line was a highly metastatic potential cell line which derived from Dunn's osteosarcoma (transplantable to C3H mouse) [19]. The KLN205 and LM8 cells were maintained in RPMI 1640 medium (Gibco BRL, Carlsbad, CA, USA) supplemented with 10% heat-inactivated fetal bovine serum (FBS; ICN Biomedicals, Inc., Aurora, OH, USA), penicillin (100 IU/ml), and streptomycin (0.1 mg/ml; Gibco BRL) in a humidified incubator at 37°C with a mixture of 5% CO_2 and 95% air.

2.2. Animals and tumor models

Female DBA/2J and C3H/HeN mice (age, 5 weeks old; weight, 18–22 g) were used throughout this study. Approximately 1×10^5 cells were inoculated subcutaneously in the shaved lower dorsum of the mice. The DBA/2J and C3H/HeN mice were inoculated with the KLN205 and LM8 cells, respectively. Tumors were obtained for experimentation at 7–12 days after inoculation when they attained a surface diameter of 6–8 mm and a thickness of 3–4 mm. The mice were generally anesthetized by an intraperitoneal administration of ketamine (75 mg/kg) and medetomidine (1.0 mg/kg), and placed on a heated water blanket throughout the treatments. All animal procedures and experiments were conducted according to the protocols approved by the Animal

Care and Use Committee of Hokkaido University.

2.3. Photosensitizer

Liposomal BPD-MA in the form of a freeze-dried powder was kindly donated by QLT Inc. (Vancouver, BC, Canada). It was reconstituted with distilled water. Stock solutions of 0.4 mg/kg BPD-MA were prepared within 24 h prior to its administration into the animals.

2.4. Photodynamic therapy

We studied the following two experimental groups: (i) a 3-h-interval PDT group (BPD-MA was administered at 3 h before laser irradiation) and (ii) a 15-min-interval PDT group (BPD-MA was administered at 15 min before laser irradiation). The tumor-bearing mice were intravenously administered approximately 0.1 ml of BPD-MA stock solution to achieve a dose of 2 mg/kg body weight, and these were irradiated with 690-nm laser light emitted by a diode laser (Coherent Japan, Inc., Tokyo, Japan). The light was delivered to the mice through a quartz fiber fitted with a microlens (Pioneer Optics, Inc, Windsor Lock, CT, USA), and expanded onto the tumor and a 2–4 mm skin margin. The tumors were exposed to an incident irradiance of 250 mW/cm^2, and the total light dose was 150 J/cm^2.

2.5. Tumor regrowth assay

The mice were assigned to the different treatment groups. The resulting treatment effect was assayed by the change in the tumor volume. The tumor size was regularly measured after PDT by using a caliper, and the tumor volume was calculated using the formula $(a \times b \times c)\ \pi/6$, where a, b, and c are three orthogonal diameters of the tumor.

2.6. Power Doppler blood flow measurements

Imaging of the mice tumors was performed using a EUB-6000 Digital Ultrasound Scanner (Hitachi Medical Co., Tokyo, Japan) with a 13 MHz transducer. The tumor was imaged in its entirety through the longest axis. Power Doppler US examinations were performed before and at 3 and 24 h after PDT. An approximately 5-mm acoustic standoff between the transducer face and the tumor was achieved by generous application of an acoustic gel. Power Doppler measurement settings were kept constant for all the tumors (46% color gain). The initial scanning of the tumor was performed in the B mode (grayscale US) to define the boundary of the tumor mass based on echogenicity parameters. Subsequently, a rectangular area was marked around the tumor and the surrounding tissue, denoting the region in which power Doppler data would be acquired. The images were stored on an optical disk in a data exchange file format. The colored area was quantified by using commercially available software (Scion Image, Scion Co., Frederick, MD, USA). A region of interest (ROI) was drawn around the entire tumor based on the initiated B-mode scan. Three measurements—the mean color level (MCL), fractional area (FA), and color-weighted FA (CWFA)—were obtained for each ROI. The MCL was obtained by dividing the sum of the integrated power values by the total number of colored pixels in the ROI; the MCL values indicated the mean density of the moving RBCs above the threshold velocity. The FA was calculated as the ratio of the colored pixels to the total number of pixels in the ROI; the FA values represented a vascularity index and indicated the percentage area of the tumor occupied by the blood vessels. The CWFA was determined as the product of the first two parameters [(MCL × FA)/100]; the CWFA indicated the blood volume within the tissue. Both MCL and CWFA were used to assess the tumor perfusion. The values of each

parameter were averaged for each tumor.

2.7. Western blot analysis

HIF-1α expression within the tumor tissue was determined by western blot analysis. The tumor-bearing animals were humanely sacrificed by intraperitoneal administration of pentobarbital sodium at a lethal overdose and cervical dislocation before and at 3 h and 24 h after PDT. The tumor tissues were then harvested and immediately frozen in liquid nitrogen. Whole cell extracts were prepared in lysis buffer containing 50 mM Hepes, 20 mM NaF, 10 mM sodium pyrophosphate, 150 mM NaCl, 2 mM $NaVO_3$, 5 mM EDTA (4Na), a complete protease inhibitor cocktail tablet (Roche Diagnostics Corp., Nutley, NJ, USA), and 1% NP-40. After the tumor tissues were homogenized with lysis buffer on ice, cell extracts were centrifuged at 16,000 × *g* for 15 min, and the supernatants were collected. Protein concentrations of the supernatants were determined by using a BCA protein assay kit (Pierce Biotechnology Inc., Rockford, IL, USA). The protein samples (30 μg) were mixed in sample buffer containing 2% sodium dodecylsulfate, 50 mM Tris-HCl (pH 6.8), 10% glycerol, and 0.01% bromophenol blue and then boiled for 3 min. The protein samples were size-separated on 10% discontinuous polyacrylamide gels and transferred to polyvinylidene difluoride membranes (Bio-Rad Laboratories, Hercules, CA, USA). The membranes were blocked overnight with 5% nonfat dry milk, which was used as a blocking solution, at 4°C and then incubated with a mouse monoclonal anti-HIF-1α antibody (Sigma-Aldrich Co., Saint Louis, MO, USA) at a 1:1,000 dilution in the blocking solution for 1 h at room temperature. Next, these membranes were incubated with an antimouse horseradish peroxidase-conjugated secondary antibody (Santa Cruz Biotechnology, Inc., Santa Cruz, CA, USA) at a 1:1,000 dilution in the blocking solution for 1 h, and the resulting

complexes were visualized by using the ECL western blotting detection kit (Amersham Biosiences Co., Piscataway, NJ, USA).

2.8. Histological examination

To examine the PDT-induced histological changes in the tumor tissue and the surrounding normal tissue, the animals were sacrificed before and at 3 h or 24 h after PDT, as described above. Tumor tissues were harvested and then fixed in 10% buffered formalin and embedded in paraffin. Tumor sections were cut to a 4 μm thickness, stained with hematoxylin & eosin (H&E), and examined under a light microscope.

2.9. Statistical analysis

The blood flow and the tumor size data were analyzed by the repeated measures of analysis of variance test, which was performed using statistical software (StatView® version 5.0; SAS Institute Inc, Cary, NC, USA). A p value <0.05 was considered statistically significant.

3. Results

3.1. Tumor regrowth measurements

Compared to the untreated group, PDT-induced significant tumor regrowth delay in both tumors was observed in the 15-min-interval PDT as well as in the 3-h-interval PDT groups ($p < 0.0001$; Fig. 1). In addition, the 15-min-interval PDT was more effective in inducing tumor regrowth delay than the 3-h-interval PDT; however, no significant difference was observed between these treatments.

In the 15-min-interval PDT group, tissue edema was observed around the irradiated area for approximately 2 days after PDT. Eschar formation was observed a

few days after PDT, and the irradiated area was cicatrized within approximately 1 week after PDT. In the case of the KLN205 tumors, the tumor was not observed from 6 to 10 days after PDT. In the case of the LM8 tumors, the tumor was not observed from 4 to 10 days after PDT. In both tumors, some tumors recurred at approximately 10 days after PDT.

In the 3-h-interval PDT group, the tumor size decreased by approximately half after PDT and increased from 4 days after PDT in both tumors. Edema and Eschar formation was not observed.

3.2. Power Doppler blood flow measurements

The tumor center appeared relatively anechoic, as illustrated by the representative images from each group (Fig. 2). In the tumors before PDT (Fig. 2A, D), the majority of the colored area was observed at the tumor periphery. In tumors at 24 h after the 15-min-interval PDT (Fig. 2B, E), the colored area almost disappeared. In tumors at 24 h after the 3-h-interval PDT (Fig. 2C, F), only a small portion of the colored area was observed in the tumor periphery.

Figure 3 shows the changes in each parameter of power Doppler US.

In the 15-min-interval PDT group, the MCLs of the KLN205 and LM8 tumors at 24 h after PDT decreased to 58.9% and 64.3% of their initial pretreatment values, respectively. In the 3-h-interval PDT group, the MCLs of the KLN205 and LM8 tumors at 24 h after PDT decreased to 75.6% and 88.2% of their initial pretreatment values, respectively. In the LM8 tumors, the transition of MCL was significantly different between the two groups ($p < 0.05$).

In the 15-min-interval PDT group, the FAs of the KLN205 and LM8 tumors at 3 h after PDT declined markedly, and the FAs of the KLN205 and LM8 tumors at 24 h after

PDT decreased to 22.2% and 13.7% of their initial pretreatment values, respectively. In the 3-h-interval PDT group, the FA of the LM8 tumors at 3 h after PDT declined markedly, and the FAs of the KLN205 and LM8 tumors at 24 h decreased to 62.8% and 60.7% of their initial pretreatment values, respectively. In the KLN205 tumors, transition of the FA was significantly different between the two groups ($p < 0.0001$).

In the 15-min-interval PDT group, the CWFAs of the KLN205 and LM8 tumors at 3 h after PDT declined markedly, and the CWFAs of the KLN205 and LM8 tumors at 24 h decreased to 14.8% and 8.0% of their initial pretreatment values, respectively. In the 3-h-interval PDT group, the CWFA of the LM8 tumors at 3 h after PDT declined markedly, and the FAs of the KLN205 and LM8 tumors at 24 h decreased to 51.2% and 53.6% of their initial pretreatment values, respectively. In the KLN205 tumors, the transition of the CWFA was significantly different between the two groups ($p < 0.05$).

3.3. HIF-1α expression

In the KLN205 and LM8 tumors, HIF-1α protein expression in the tumor tissues after the 15-min-interval PDT and the 3-h-interval PDT was observed (Fig. 4). In the 15-min-interval PDT group, the level of HIF-1α expression in the KLN205 tumors was less at 3 h after PDT; however, it increased by 24 h after PDT. In the 15-min-interval PDT group, no difference was observed in the level of HIF-1α expression in the LM8 tumors at 3 h and 24 h after PDT. In the 3-h-interval PDT group, the level of HIF-1α expression in both tumors was greater at 3 h after PDT; however, it decreased by 24 h after PDT. Compared to the 3-h-interval PDT, the 15-min-interval PDT induced a greater level of HIF-1α expression in the KLN205 tumors.

3.4. Histological examination

A histological examination of untreated tumors showed tumor cells with intact blood vessels. The red blood cells were visible within the lumen (Fig. 5A, F).

At 3 h after the 15-min-interval PDT, the blood vessels were dilated and congested with red blood cells, and hemorrhage caused by the rupture of blood vessels could also be detected (Fig. 5B, G). At 24 h after the 15-min-interval PDT, edema and hemorrhage were more severe and extensive. The tumor cells appeared pyknotic and were separated from each other (Fig. 5C, H). Cell death was observed around the damaged vasculature, and a small number of viable tumor cells were observed at the tumor periphery.

Congested blood vessels and hemorrhage were also observed at 3 h after the 3-h-interval PDT; however, the extent of congestion and hemorrhage was lesser than that observed in the 15-min-interval PDT group. Pyknosis and cell separation induced by the 3-h-interval PDT was more extensive than that induced by the 15-min-interval PDT (Fig. 5D, I). By 24 h after the treatment, cell death was observed in the entire tumor, except the peripheral tumor cells that were viable (Fig. 5E, J).

4. Discussion

The biological target of PDT using BPD-MA depends on the interval between drug injection and light irradiation. PDT with a short drug-light interval (15-min-interval PDT) targets tumor vasculature, whereas PDT with a long drug-light interval (3-h-interval PDT) targets cellular compartments [5]. In a previous study using Meth A sarcoma-bearing mice, 15-min-interval PDT suppressed tumor growth and prolonged the survival time to a greater extent than 3-h-interval PDT [5]. In the present study, we chose different two types of cell line. KLN205 tumor was mouse lung squamous cell carcinoma. LM8 tumor was mouse osteosarcoma. The 15-min-interval

PDT was more effective than the 3-h-interval PDT (Fig. 1). The 15-min-interval PDT cuts off the supply of nutrients and oxygen those are necessary for neoplastic tissues [5]; therefore, it might be potentially effective in destroying the vasculature in solid tumors.

In studies using tumor-bearing mice, Doppler US has proved to be a valuable noninvasive method for serial examinations of the vascularity and perfusion within the tumor during antiangiogenic treatment and radiation therapy [20-22]. Power Doppler US records the amplitude (energy) of the Doppler signal reflected from the moving blood cells and was sensitive for detecting low velocities and parenchymal vessels as small as 15–20 μm in diameter [23]. Due to the typically high interstitial pressure in tumors and resultant low-velocity states in tumor vessels, power Doppler US is of special value in assessing tumor vasculature. In addition, a significantly positive correlation has been reported between Doppler blood flow and microvessel density measurements [20]. Therefore, we investigated whether the effects of PDT could be evaluated using the tumor vascularity and perfusion data, which were determined by power Doppler US.

It was reported that the blood flow values in control groups such as the BPD-MA alone group, the light alone group, and the no drug and no light group were slightly higher than the pretreatment values [24]. In the KLN205 tumors, the transition of the FA and the CWFA was significantly different between the 15-min-interval PDT and the 3-h-interval PDT groups (Fig. 3). This difference could be due to the loss of small vessels (<300 μm^2) that was largely responsible for the reduction in the FA, which in turn is responsible for the decrease in the CWFA [20]. It was considered that the progressive decreases in the PDT-induced CWFA and FA values provided unequivocal evidence of therapeutic response. In the LM8 tumors, the transition of the MCL was significantly different between the 15-min-interval PDT and the 3-h-interval PDT

groups. These results indicated that compared to the 3-h-interval PDT, the 15-min-interval PDT induced a significantly higher decrease in the tumor vascularity (based on the FA measurement) and perfusion (based on the MCL and CWFA measurements). However, the 3-h-interval PDT also damaged the vasculature to a small extent. It was reported that radiation-induced fibrosarcoma-1 tumors were exposed to laser light at either 0.5 h or 6 h after a 5 mg/kg dose of hypericin. A complete arrest of vascular perfusion was detected by 15 h after the 0.5 h-interval PDT, whereas well-perfused areas could still be found at this time in tumors after the 6-h interval PDT [25]. The reported results were similar to our present results.

Power Doppler US is considered to be assessed the efficacy of PDT conveniently, safely, and repeatedly. However, this technique has some limitations in that the results may vary depending on the operator, as in the case of any US technique [12]. Power Doppler US is subject to motion artifacts due to the transducer, which can simulate blood flow. The study of deeper organs might also be more limited by motion artifacts due to adjacent respiratory or heart motion. Moreover, the analysis of the images is subject to variability depending on the manner in which the ROI are drawn and the tumor is framed within the analysis software [12]. In this study, therefore, we attempted to minimize motion artifacts and center the tumor image in the power Doppler US box, and the ROI was drawn to include only the tumor.

Hypoxia-inducible factor-1 is a heterodimeric complex of two helix-loop-helix proteins, HIF-1α and HIF-1β (ARNT) [17]. ARNT is constitutively expressed, whereas HIF-1α is rapidly degraded under normoxic conditions by the ubiquitin-proteasome system [14,16,26]. Hypoxia induced the stabilization of the HIF-1α subunit protein. This protein is a major regulator of the hypoxic response of tumor cells. After hypoxic stabilization, HIF-1α translocates to the nucleus, forms the HIF-1 dimer with the

ubiquitous HIF-1β, and subsequently binds to the hypoxia-responsive elements of hypoxia-regulated genes such as vascular endothelial growth factor (VEGF), erythropoietin, or glucose transporters [17].

We detected the time course of HIF-1α protein expression in each tumor after PDT. In both tumors, the level of HIF-1α expression at 3 h after the 3-h-interval PDT was high. It was believed that the photodynamic reaction induced the consumption of oxygen by cells and rapidly caused hypoxia of the entire tumor tissue because the 3-h-interval PDT targeted the cellular compartment [24,27]. At 24 h after the 3-h-interval PDT, a number of tumor cells were killed, and the level of HIF-1α expression decreased although the blood flow in the tumor persisted (Fig. 3). On the other hand, at 3 h after PDT, the level of HIF-1α expression induced by the 15-min-interval PDT was lesser than that induced by the 3-h-interval PDT although the blood flow in the tumor decreased remarkably (Fig. 3). This was believed to be due to the hypoxia that was induced only around the damaged vasculature and not in the entire tumor tissue because the 15-min-interval PDT mainly targeted the tumor vasculature [24]. With regard to the level of HIF-1α expression, it was believed that at 24 h after the 15-min-interval PDT, the hypoxia area occurring due to vessel rupture (Fig. 5C, H) gradually increased within the tumor tissue. The difference in HIF expression after 15-min-interval PDT between both cell lines was considered to be related to the change of the MCL (Fig. 2A, C). It was possible that PDT-induced tumor tissue hypoxia could stabilize HIF-1α and initiate HIF-1-mediated transcription.

HIF-1α could regulate the expression of genes not only involved in angiogenesis but also those that contribute to tumor cell survival and aggressiveness [17,28]. Palayoor et al. reported that one of the effects of nonsteroidal anti-inflammatory drugs (NSAIDs) was to reduce the level of HIF protein expression [29]. The level of HIF-1α

expression was high at 3 h after the 3-h-interval PDT; therefore, the use of NSAIDs might have an effect on the suppression of tumor recurrence as well as neovascularization stimulated by VEGF after the 3-h-interval PDT.

To confirm the effects of PDT, we performed histological examination of the tumor tissues. At 24 h after the 3-h-interval PDT, cell death was observed in the entire tumor, except the peripheral tumor cells. Therefore, there was a possibility of this tumor recurring because the tumor cells and vasculature remained intact at the tumor periphery. In the 15-min-interval PDT group, the dead cells showed condensed nuclei, a characteristic of apoptotic cell death, around the damaged and ruptured tumor vasculature. It was also reported that vasculature-targeting PDT induced apoptotic cell death [30,31]. It was indicated the dominant intravascular localization of the photosensitizer with slight diffusion beyond the boundaries [31]. Therefore, the tumor cells were directly damaged by photodynamic effect surrounding the tumor vasculature. Although the 3-h-interval PDT induced more extensive cell death than the 15-min-interval PDT at 3 h after PDT, both PDT treatments resulted in a similar extent of cell death at 24 h after PDT. It was reported that these differences might be due to the difference in the stages of cell death induced by the 15-min-interval PDT and the 3-h-interval PDT [30]. The histological findings such as vascular rupture and hemorrhage indicating vascular damage might be associated with those of hemodynamics observed during power Doppler US analysis. In the 3-h-interval PDT, power Doppler US examination detected the vascularity at the tumor periphery. This difference in response implied that the vasculature in the tumor center might be more sensitive to PDT-induced vascular damage than that in the tumor periphery and in the surrounding tissue [25].

In our *in vitro* study using propidium iodide staining, a significant difference in

the proportion of apoptosis was observed between the KLN205 cells and the LM8 cells [32]. In this study, however, no significant difference in the delay in tumor regrowth was observed between the KLN205 and the LM8 tumors treated by the 3-h-interval PDT. These differences in the results of the *in vitro* and *in vivo* study might be due to the difference in the experimental condition and influence of several factors in the tumor tissue, such as photosensitizer uptake, tissue oxygen concentration, light dose delivered, etc [3,33,34].

In a previous study using mammary tumors (MCaIV tumors), combining cellular and vasculature-targeting PDT (the photosensitizer was injected at 4 h and 15 min before laser irradiation) induced tumor growth delay more effectively than when cellular- or vasculature-targeting PDT were used alone [35]. In our study using the KLN205 tumors, combining the 3-h-interval and the 15-min-interval PDT also resulted in a more drastic tumor regression than when each PDT was used alone (data not shown). During the experimental period of 21 days, the tumor did not recur. Therefore, a combination of the cellular- and vasculature-targeting PDT has the potential to become a new and more effective treatment method for tumors.

In the present study, hypoxia was induced more rapidly in the entire tumor after the 3-h-interval PDT (cellular-targeting PDT) than after the 15-min-interval PDT (vasculature-targeting PDT). However, compared to the 3-h interval PDT, the 15-min-interval PDT induced tumor growth delay more effectively. Therefore, it was considered that vasculature-targeting PDT was effective in destructing the vasculature in solid tumors. It was also considered that power Doppler US could assess the efficacy of PDT conveniently, safely, and repeatedly.

5. Acknowledgement

We thank QLT, Inc. (Vancouver, British Columbia, Canada) for donating BPD-MA. This work was supported by a Grant-in Aid from the Ministry of Education, Culture, Sport, Science and Technology of Japan (15380211).

6. Reference

[1] Y. N. Konan, R. Gurny, E. Allémann, State of the art in the delivery of photosensitizers for photodynamic therapy, J. Photochem. Photobiol. B 66 (2002) 89-106.

[2] M. B. Vrouenraets, G. W. Visser, G. B. Snow, G. A. van Dongen, Basic principles, applications in oncology and improved selectivity of photodynamic therapy, Anticancer Res. 23 (2003) 505-522.

[3] T. J. Dougherty, C. J. Gomer, B. W. Henderson, G. Jori, D. Kessel, M. Korbelik, J. Moan, Q. Peng, Photodynamic therapy, J. Natl. Cancer Inst. 90 (1998) 889-905.

[4] W. M. Sharman, C. M. Allen, J. E. van Lier, Photodynamic therapeutics: basic principles and clinical applications, Drug Discov. Today 4 (1999) 505-517.

[5] K. Kurohane, A. Tominaga, K. Sato, J. R. North, Y. Namba, N. Oku, Photodynamic therapy targeted to tumor-induced angiogenic vessels, Cancer Lett. 167 (2001) 49–56.

[6] V. H. Fingar, P. K. Kik, P. S. Haydon, P. B. Cerrito, M. Tseng, E. Abang, T. J. Wieman, Analysis of acute vascular damage after photodynamic therapy using benzoporphyrin derivative (BPD), Br. J. Cancer 79 (1999) 1702-1708.

[7] K. Shimizu, N. Oku, Cancer anti-angiogenic therapy, Biol. Pharm. Bull. 27 (2004) 599-605.

[8] T. H. Foster, R. S. Murant, R. G. Bryant, R. S. Knox, S. L. Gibson, R. Hilf, Oxygen consumption and diffusion effects in photodynamic therapy, Radiat. Res. 126 (1991) 296-303.

[9] V. H. Fingar, T. J. Wieman, S. A. Wiehle, P. B. Cerrito, The role of microvascular damage in photodynamic therapy: the effect of treatment on vessel constriction, permeability, and leukocyte adhesion, Cancer Res. 52 (1992) 4914-4921.

[10] I. P. van Geel, H. Oppelaar, P. F. Rijken, H. J. Bernsen, N. E. Hagemeier , A. J. van der Kogel, R. J. Hodgkiss, F. A. Stewart, Vascular perfusion and hypoxic areas in RIF-1 tumours after photodynamic therapy, Br. J. Cancer 73 (1996) 288-293.

[11] T. M. Sitnik, J. A. Hampton, B. W. Henderson, Reduction of tumour oxygenation during and after photodynamic therapy in vivo: effects of fluence rate, Br. J. Cancer 77 (1998) 1386-1394.

[12] E. F. Donnelly, L. Geng, W. E. Wojcicki, A. C. Fleischer, D. E. Hallahan, Quantified power Doppler US of tumor blood flow correlates with microscopic quantification of tumor blood vessels, Radiology 219 (2001) 166-170.

[13] A. L. Vavere, J. S. Lewis, Imaging the effects of anti-angiogenic treatments, Q. J. Nucl. Med. 47 (2003) 163-170.

[14] P. J. Ratcliffe, J. F. O'Rourke, P. H. Maxwell, C. W. Pugh, Oxygen sensing, hypoxia-inducible factor-1 and the regulation of mammalian gene expression, J. Exp. Biol. 201 (1998) 1153-1162.

[15] A. Ferrario, K. F. von Tiehl, N. Rucker, M. A. Schwarz, P. S. Gill, C. J. Gomer, Antiangiogenic treatment enhances photodynamic therapy responsiveness in a mouse mammary carcinoma, Cancer Res. 60 (2000) 4066-4069.

[16] G. L. Wang, G. L. Semenza, General involvement of hypoxia-inducible factor 1 in transcriptional response to hypoxia, Proc. Natl. Acad. Sci. USA 90 (1993) 4304-4308

[17] J. A. Forsythe, B. H. Jiang, N. V. Iyer, F. Agani, S. W. Leung, R. D. Koos, G. L. Semenza, Activation of vascular endothelial growth factor gene transcription by hypoxia-inducible factor 1, Mol. Cell Biol. 16 (1996) 4604-4613.

[18] T. Kaneko, G. A. LePage, T. K. Shnitka, KLN205 – a murine lung carcinoma cell line, In Vitro 16 (1980) 884-892.

[19] T. Asai, T. Ueda, K. Itoh, K. Yoshioka, Y, Aoki, S. Mori, H. Yoshikawa, Establishment and characterization of a murine osteosarcoma cell line (LM8) with high metastatic potential to the lung, Int. J. Cancer 76 (1998) 418-422.

[20] M. S. Gee, H. M. Saunders, J. C. Lee, J. F. Sanzo, W. T. Jenkins, S. M. Evans, G. Trinchieri, C. M. Sehgal, M. D. Feldman, W. M. Lee, Doppler ultrasound imaging detects changes in tumor perfusion during antivascular therapy associated with vascular anatomic alterations, Cancer Res. 61 (2001) 2974-2982.

[21] F. Denis, P. Bougnoux, L. de Poncheville, M. Prat, R. Catroux, F. Tranquart, In vivo quantitation of tumour vascularisation assessed by Doppler sonography in rat mammary tumours, Ultrasound Med. Biol. 28 (2002) 431-437.

[22] F. Denis, S. Colas, L. Chami, P. Louisot, O. Le Floch, F. Tranquart, P. Bougnoux, Changes in tumor vascularization after irradiation, anthracyclin, or antiangiogenic treatment in nitrosomethyl ureas-induced rat mammary tumors, Clin. Cancer Res. 9 (2003) 4546-4552.

[23] D. E. Goertz, D. A. Christopher, J. L. Yu, R. S. Kerbel, P. N. Burns, F. S. Foster, High-frequency color flow imaging of the microcirculation, Ultrasound Med. Biol. 26 (2000) 63-71.

[24] B. Chen, B. W. Pogue, I. A. Goodwin, J. A. O'Hara, C. M. Wilmot, J. E. Hutchins, P. J. Hoopes, T. Hasan, Blood flow dynamics after photodynamic therapy with Verteporfin in the RIF-1 tumor, Radiat. Res. 160 (2003) 452-459.

[25] B. Chen, T. Roskams, P. A. de Witte, Antivascular tumor eradication by Hypericin-mediated photodynamic therapy, Photochem. Photobiol. 76 (2002a) 509-513.

[26] L. E. Huang, J. Gu, M. Schau, H. F. Bunn, Regulation of hypoxia–inducible factor 1alpha is mediated by an O_2-dependent degradation domain via the

ubiquitin-proteasome pathway, Proc. Natl. Acad. Sci. USA 95 (1998) 7987-7992.

[27] A. P. Castano, T. N. Demidova, M. R. Hamblin, Mechanisms in photodynamic therapy: part one - photosensitizers, photochemistry and cellular localization, Photodiag. Photodynam. Ther. 1 (2004) 279-293.

[28] H. Axelson, E. Fredlund, M. Ovenberger, G. Landberg, S. Pahlman, Hypoxia-induced dedifferentiation of tumor cells - a mechanism behind heterogeneity and aggressiveness of solid tumors, Semin. Cell Dev. Biol. 16 (2005) 554-563.

[29] S. T. Palayoor, P. J. Tofilon, C. N. Coleman, Ibuprofen-mediated reduction of hypoxia-inducible factors HIF-1α and HIF-2α in prostate cancer cells, Clin. Cancer Res. 9 (2003) 3150-3157.

[30] B. Chen, T. Roskams, Y. Xu, P. Agostinis, P. A. de Witte, Photodynamic therapy with hypericin induces vascular damage and apoptosis in the RIF-1 mouse tumor model, Int. J. Cancer 98 (2002b) 284-290.

[31] B. Chen, B. W. Pogue, P. J. Hoopes, T. Hasan, Combining vascular and cellular targeting regimens enhances the efficacy of photodynamic therapy, Int. J. Radiat. Oncol. Biol. Phys. 61 (2005) 1216-1226.

[32] T. Osaki, S. Takagi, Y. Hoshino, M. Okumura, T. Fujinaga, Intracellular localization and concentration as well as photodynamic effects of benzoporphyrin derivative monoacid ring A in four types of rodent tumor cells, Cancer Lett. (2006) in press.

[33] Z. Huang, Q. Chen, A. Shakil, H. Chen, J. Beckers, H. Shapiro, F. W. Hetzel, Hyperoxygenation enhances the tumor cell killing of photofrin-mediated photodynamic therapy, Photochem. Photobiol. 78 (2003) 496-502.

[34] C. Sheng, B. W. Pogue, E. Wang, J. E. Hutchins, P. J. Hoopes, Assessment of

photosensitizer dosimetry and tissue damage assay for photodynamic therapy in advanced-stage tumors, Photochem. Photobiol. 79 (2004) 520-525.

[35] D. E. Dolmans, A. Kadambi, J. S. Hill, K. R. Flores, J. N. Gerber, J. P. Walker, I. H. Borel Rinkes, R. K. Jain, D. Fukumura, Targeting tumor vasculature and cancer cells in orthopedic breast tumor by fractionated photosensitizer dosing photodynamic therapy, Cancer Res. 62 (2002) 4289-4294.

Figure legends

Fig. 1. Changes in tumor volume in response to PDT using BPD-MA.

A: KLN205 tumors (n = 6). B: LM8 tumors (n = 5). ◆: untreated tumor group (n = 6). △: 3-h-interval PDT group. ■: 15-min-interval PDT group. In both tumors, the 15-min-interval PDT group or the 3-h-interval PDT group significantly induced tumor regrowth delay when compared with the untreated tumor group ($p < 0.0001$). Error bars show the standard error for these mean values.

Fig. 2. Power Doppler ultrasound images of the KLN205 tumors (n = 5) and LM8 tumors (n = 6) before and after PDT. A–C: KLN205 tumors. D–F: LM8 tumors. A, D: before PDT. B, E: at 24 h after the 15-min-interval PDT. C, F: at 24 h after the 3-h-interval PDT. In each image, the tumor center appears relatively anechoic, and the regions with blood flow are depicted in color. One of representative tumor images of each group was shown.

Fig. 3. Changes in the power Doppler ultrasonographic parameters for assessing the vascularity and the perfusion after PDT. ■: mean color level (MCL), ◇: fractional area (FA), and ▲: color-weighted fractional area (CWFA). A, B: KLN205 tumors (n = 5). C, D: LM8 tumors (n = 6). A, C: the 15-min-interval PDT group. B, D: the 3-h-interval PDT group. In the KLN205 tumors, the transition of the FA and CWFA was significantly different between the 15-min-interval PDT and the 3-h-interval PDT groups ($p < 0.0001$ and $p < 0.05$, respectively). In the LM8 tumors, the transition of MCL was significantly different between the 15-min-interval PDT and the 3-h-interval PDT groups ($p < 0.05$). Error bars show the standard error for these mean values.

Fig. 4. Tumors were collected after PDT and evaluated for HIF-1α expression by western blot analysis. PDT treatment induced HIF-1α expression in both tumors (n = 3). HIF-1α expression was not detectable in control tumors (untreated tumors). In the KLN205 tumors, the level of HIF-1α expression was low at 3 h after the 15-min-interval PDT; however, it increased by 24 h after PDT. No difference was observed in the level of HIF-1α expression between the LM8 tumors at 3 h and 24 h after PDT. In both tumors, the level of HIF-1α expression was high at 3 h after the 3-h-interval PDT; however, it decreased at 24 h after PDT. The level of HIF-1α expression induced in the KLN205 tumors at 3 h after the 15-min-interval PDT was greater than that induced by the 3-h-interval PDT. One of representative tumor HIF-1α results of each group was shown.

Fig. 5. Representative H&E stained images of the KLN205 tumors (n = 3) and LM8 tumors (n = 3) after PDT. A, F: untreated tumors (tumor cells with intact blood vessels and red blood cells are visible within the lumen). B, G: at 3 h after the 15-min-interval PDT (ruptured, dilated, and congested blood vessels are observed). C, H: at 24 h after the 15-min-interval PDT (tumor cells appear pyknotic and are separated from each other). D, I: at 3 h after the 3-h-interval PDT (tumor cells appear pyknotic and are separated from each other). E, J: at 24 h after the 3-h-interval PDT (a rim of viable cells is found at the tumor periphery). Arrows indicate the dilated and ruptured vasculature. Asterisks indicate the viable tumor cells (*). Scale bar = 100μm. One of representative tumor histological H&E stained specimens of each group was shown.

A

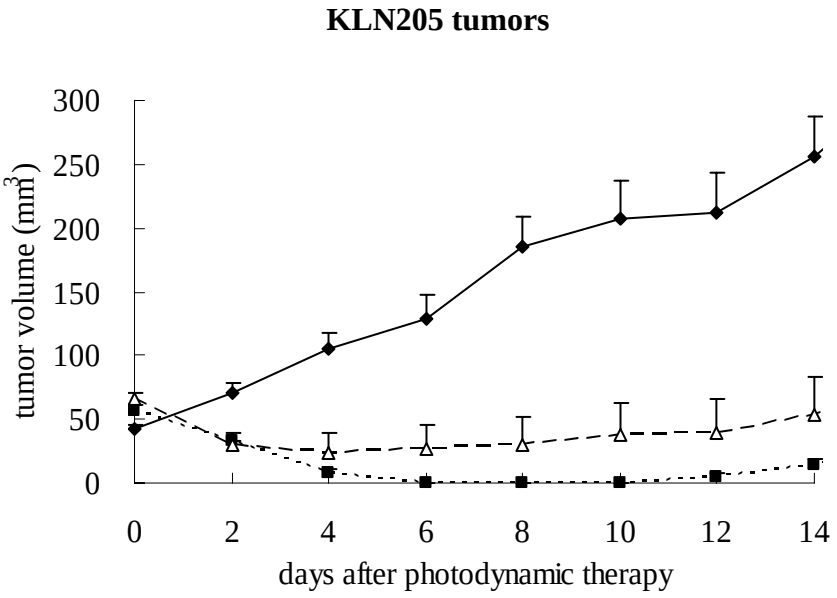
KLN205 tumors
tumor volume (mm3)
300
250
200
150
100
50
0
0
2
4
6
8
10
12
14
days after photodynamic therapy

B

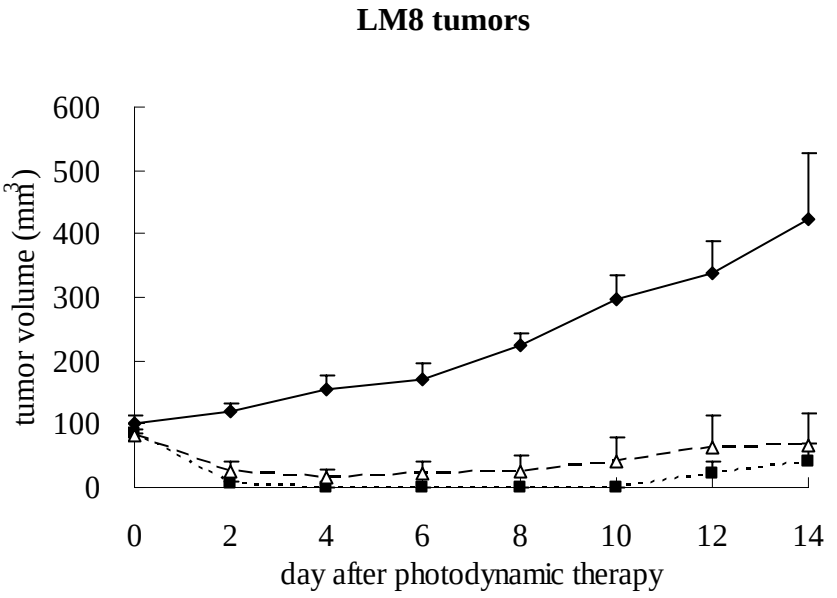
LM8 tumors
tumor volume (mm3)
600
500
400
300
200
100
0
0
2
4
6
8
10
12
14
day after photodynamic therapy

Fig. 1.

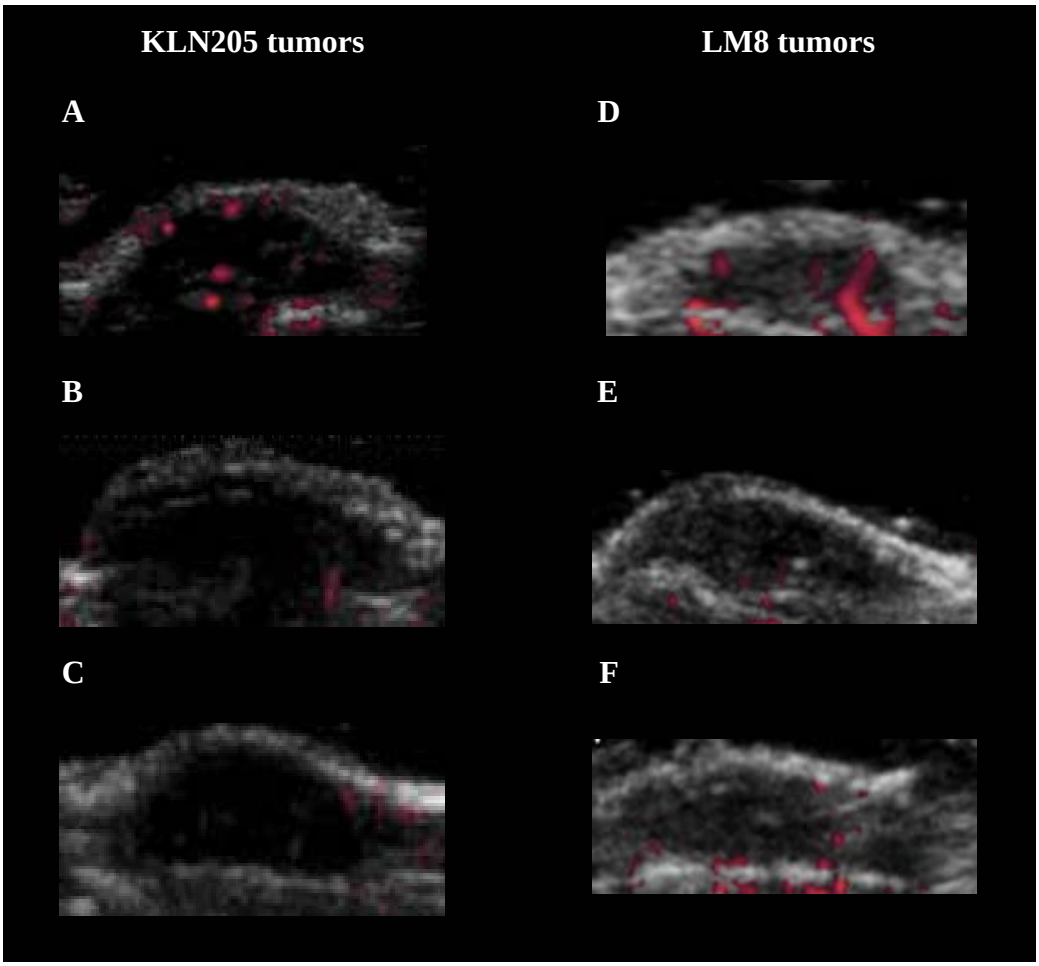

Fig. 2.

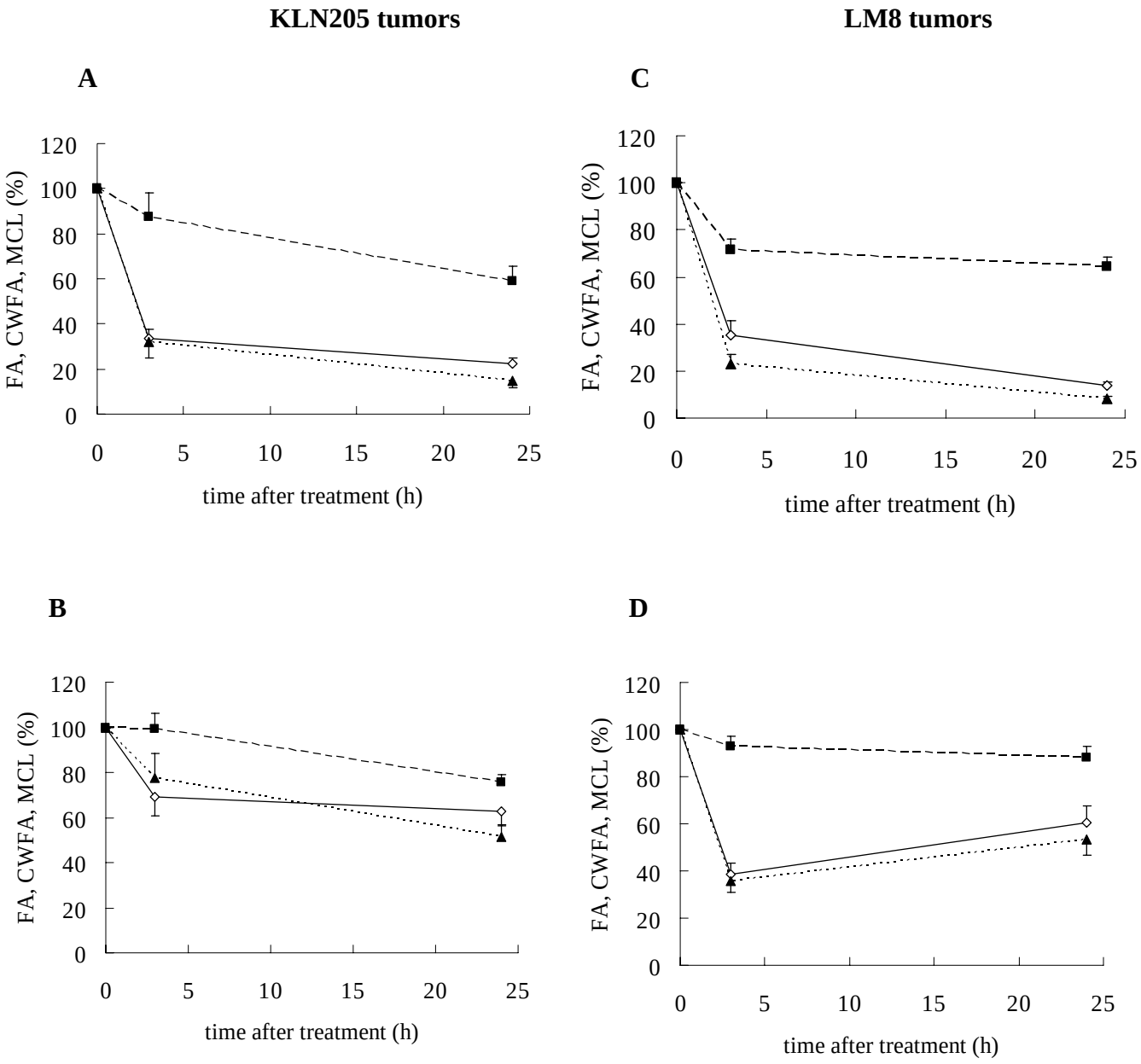
KLN205 tumors
LM8 tumors
A
B
C
D
FA, CWFA, MCL (%)
time after treatment (h)
0
20
40
60
80
100
120
0
5
10
15
20
25

Fig. 3.

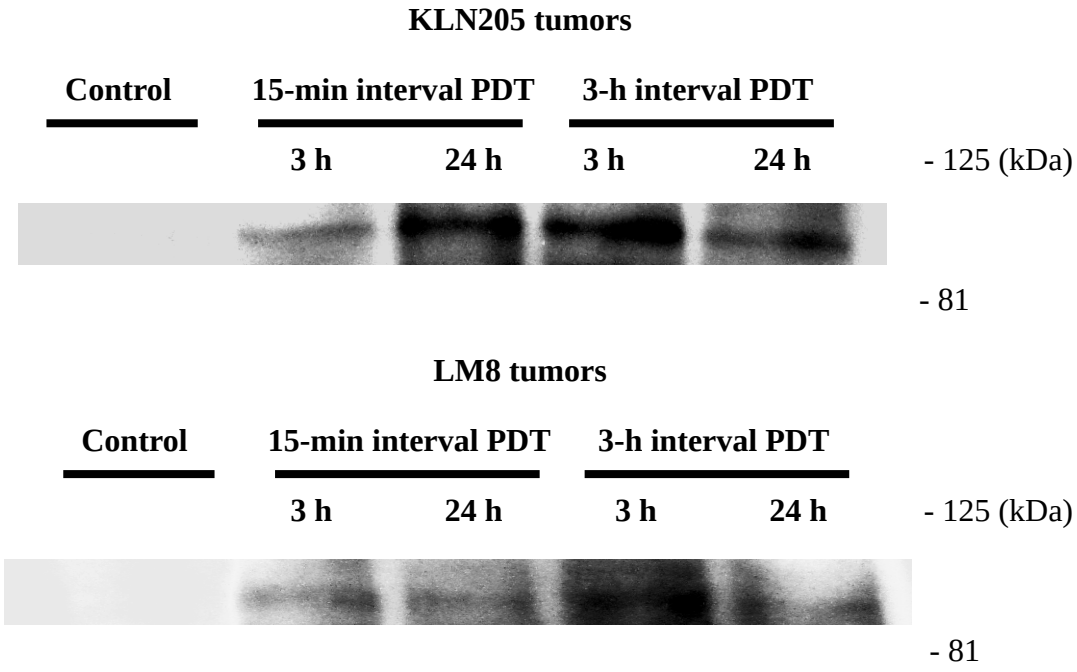
KLN205 tumors
Control
15-min interval PDT
3-h interval PDT
3 h
24 h
3 h
24 h
- 125 (kDa)
- 81
LM8 tumors
Control
15-min interval PDT
3-h interval PDT
3 h
24 h
3 h
24 h
- 125 (kDa)
- 81

Fig. 4.

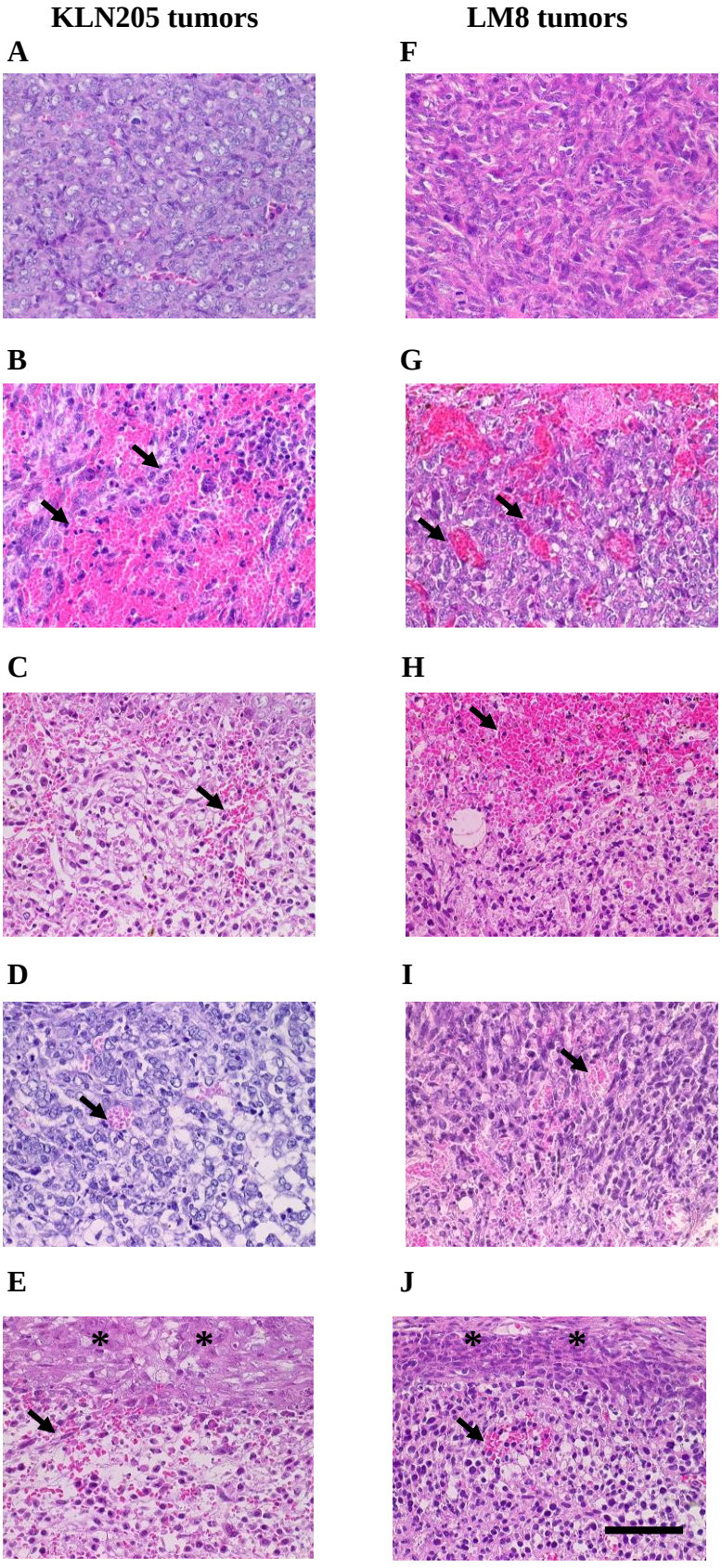

Fig. 5.